

Use of the Lognormal Distribution Function To Describe Orientational Relaxation in Optically Nonlinear Polymers

T. Verbiest,[†] D. M. Burland,* and C. A. Walsh[‡]

IBM Research Division, Almaden Research Center, 650 Harry Road,
San Jose, California 95120-6099

Received February 2, 1996; Revised Manuscript Received July 2, 1996[®]

ABSTRACT: Second harmonic generation decay has been used to follow the orientational relaxation of dipolar chromophores either dissolved in (guest–host) or chemically attached to (side chain) an amorphous polymer host. The guest–host system investigated is the chromophore lophine-1 in a polyimide host and the side-chain system is the dye molecule Disperse Red 1 chemically attached to a poly(methyl methacrylate) backbone. The relaxation at any given temperature is characterized by a functional form arising from a lognormal distribution of relaxation times. From the temperature dependence of the parameters in this function, we can obtain activation enthalpies and entropies for the relaxation process in these two polymer systems. These quantities can be related to other quantities such as the isobaric coefficient of thermal volume expansion and the activated volume. Also investigated is the effect of aging on the relaxation process.

I. Introduction

During the last decade, numerous studies of the orientational decay of second-order nonlinear optical chromophores imbedded in polymer matrices have been reported.¹ These chromophores may either be dissolved in a polymer host (guest–host systems) or covalently attached to the backbone of the polymer. If the chromophore is appended to the chain, the covalently bonded chromophore–polymer system is frequently referred to as a side-chain system. To obtain a macroscopic medium with second-order nonlinear optical (NLO) properties, the dipolar chromophores are aligned in the polymer by external electric field poling at or near the polymer glass transition temperature T_g . In the absence of the poling field, however, the polymer will slowly lose its nonlinearity as the chromophores reorient to the isotropic equilibrium state. This poled-order decay can be conveniently monitored by following the decay of the second harmonic generation (SHG) resulting from the orientation of the NLO chromophores.^{2–4} The study of such relaxation processes with SHG is both a critical tool for evaluating the utility of NLO polymers in practical applications and a powerful experimental technique for investigating the physics of polymer dynamics at temperatures below T_g and over many orders of magnitude in time.

It is commonly observed that poled-order decay in a polymer matrix below T_g deviates significantly from exponentiality, implying a complex underlying relaxation process. This nonexponential decay behavior has been described by a variety of functional forms, with the Kohlrausch–Williams–Watts (KWW)⁵ or stretched exponential function being the most widely used.^{4,6} Other functions used to describe this decay have included a sum of two exponentials,^{2,7} a sum of two stretched exponentials,⁸ a combination of exponential and stretched exponential,⁹ and a sum of a stretched exponential and a constant.¹⁰ Experimental decay data are rarely collected over a wide enough time range to

make an unambiguous distinction among these various functional forms, primarily because the length of time required to make such a distinction becomes unrealistically long the further one moves away from T_g . This is a well-known problem in the study of amorphous systems and it occurs in both time and frequency domain studies.¹¹ Recently, Torkelson and co-workers¹² have extended the time over which SHG decays have been measured to shorter times in a variety of guest–host polymer systems and used the stretched exponential function to describe the decay. The stretched exponential function is given by

$$\Phi(t) = \frac{d(t)}{d(0)} = \left(\frac{I(t)}{I(0)} \right)^{1/2} = \exp[-(t/\tau_{\text{KWW}})^{\beta_{\text{KWW}}}] \quad (1)$$

where $I(t)$ is the SHG intensity at time t and $d(t)$ is the second harmonic coefficient.¹³ The great advantage of eq 1 over many other functional forms for fitting experimental decay data is its simple analytical form and the fact that it requires only two parameters to describe the normalized decay, τ_{KWW} , the time it takes the decay to reach 1/e of its value at $t = 0$, and β_{KWW} , a quantity indicating how much the decay rate “slows” down with time. As a result, a variety of microscopic models have been proposed to identify the origin of this functional form.^{14,15}

In order to attribute physical meaning to the parameters that arise from any of these decay functions, one must be confident that the decay function itself correctly describes the data. Since, in practice, for measurements below T_g , it is often not possible to follow the decay over a wide enough dynamic range in $\Phi(t)$, one must look for other ways of discriminating among the various functional forms. One way of doing this is by studying the temperature dependence of the fitting parameters associated with a given functional form. This implies of course that the model in question is described by physically meaningful parameters with predictable temperature dependences. This is certainly the case for a functional form that has been used recently to describe SHG-relaxation and isomerization processes in polymers.^{16,17} In this model the relaxation process is associated with a Gaussian distribution in the logarithm of the relaxation times, which in turn arises from a Gaussian distribution of activation free energy barriers.

[†] Current address: K. U. Leuven, Department of Chemistry, Celestijnenlaan 200D, B-3001 Heverlee, Belgium.

[‡] Current address: Corporate Technology Division, Raychem Corp., 300 Constitution Dr., Menlo Park, CA 94025.

[®] Abstract published in *Advance ACS Abstracts*, August 15, 1996.

This functional decay form is referred to as the Wagner or lognormal function.^{18,19} In this paper we will show that orientational relaxation in both guest–host and side-chain polymer systems can be described by using the Wagner function. We will attempt to describe the temperature dependence and the effect of physical aging on the relaxation parameters of the Wagner model and compare the predictions from this model with experimental results on both guest–host and side-chain NLO polymers. In addition we will calculate activation entropies, enthalpies, and thermal expansion coefficients from the temperature dependence of the relaxation parameters.

II. Lognormal Distribution (Wagner) Function¹⁹

The normalized second harmonic decay may be considered to arise from a continuous distribution of exponential relaxation times:

$$\Phi(t) = \int_{-\infty}^{\infty} \Psi(\ln \tau) \exp(-t/\tau) d \ln \tau \quad (2)$$

The normalized distribution function in the log of the relaxation times, $\Psi(\ln \tau)$ (a lognormal distribution), is, in this model, given by

$$\Psi(\ln \tau) = \frac{1}{\sigma_G \sqrt{\pi}} \exp(-u^2) \quad (3)$$

where $u = (\ln(\tau/\tau_m))/\sigma_G$. σ_G is the half-width of the Gaussian distribution at the point where $\Psi(\ln \tau)$ has fallen to $1/e$ of its maximum value. τ_m is the most probable relaxation time, corresponding to the value of τ at the maximum of the Gaussian distribution. Substituting eq 3 into eq 2, one obtains

$$\Phi(t) = \frac{1}{\sqrt{\pi}} \int \exp(-u^2) \exp(-xe^{-\sigma_G u}) du \quad (4)$$

where $x = t/\tau_m$. Equation 4 is sometimes referred to as the “after-effect function”. This integral cannot be solved analytically and must be evaluated numerically. Tabulations of the integral have been made.^{19,20} Like the stretched exponential function, this function requires only two variables, τ_m and σ_G , to fit the experimental decay data.

In order to evaluate the temperature dependence of τ_m and σ_G , certain assumptions must be made concerning the underlying mechanisms responsible for the relaxation processes under investigation. Assuming that the relaxation process below T_g is described by a distribution of thermally activated processes, the relationship between an individual τ and the temperature T can be expressed in terms of an Arrhenius equation:

$$\ln(\tau) = \ln(\tau_0) + E/RT \quad (5)$$

where τ_0 is a constant, E is an activation energy, and R is the molar gas constant. This was the temperature dependence for τ assumed in a previous study of relaxation processes in polymers.¹⁷

Alternatively, one can use an expression derived from Eyring's absolute reaction rate theory:²¹

$$\ln(\tau) = \ln(2\pi h/kT) - \Delta S/R + \Delta H/RT \quad (6)$$

with ΔS and ΔH the activation entropy and enthalpy, respectively. Both quantities are usually assumed to be temperature independent. The relationship between

the activation energy determined experimentally from eq 5 and the activation enthalpy determined from eq 6 is²²

$$E = \Delta H + RT \quad (7)$$

This expression can be shown by comparing the value of the slope obtained from a plot of $\ln(\tau)$ vs $1/T$ using eq 5 to one obtained from a plot of $\ln(\tau T)$ vs $1/T$ using eq 6. Frequently, $\Delta H \gg RT$, so that, in many cases, $E \approx \Delta H$.

In the following analysis we will use the Eyring equation (eq 6) to investigate the temperature dependence of the relaxation parameters τ_m and σ_G , because it permits one to use familiar thermodynamic variables, entropy and enthalpy, to characterize the relaxation process. We will show below that these quantities can in turn be related, in an interesting way, to quantities such as the thermal expansion coefficient. However, one cannot distinguish between eqs 5 and 6 simply from measurements of the temperature dependence of the relaxation process. In ref 17 we have in fact used eq 5 to interpret experimental data.

From eq 6 it is clear that the resulting distribution in τ must be due to either a distribution in ΔS , in ΔH , or in both quantities. In order to obtain a relationship between σ_G and the distribution widths of ΔS and ΔH , one can use the following, easily demonstrated theorem:¹⁹ *If two variables x and y are linearly related, i.e. $x = ay + b$, and if the values of x have a Gaussian distribution, then the values of y will also be distributed in a Gaussian manner, with distribution widths*

$$\sigma_y = \sigma_x/|a| \quad (8)$$

and most probable value

$$y_m = (x_m - b)/a \quad (9)$$

First consider a distribution in ΔS alone. According to the above theorem, $\sigma_G = \sigma_S/R$, where σ_S is the distribution parameter for a Gaussian distribution around a mean activation entropy ΔS_m . In this case, σ_G is temperature independent. When one considers a distribution in ΔH alone, $\sigma_G = \sigma_H/RT$, where σ_H is the distribution parameter for a Gaussian distribution around the most probable activation enthalpy ΔH_m . A plot of σ_G vs $1/T$ would, in this case, yield a straight line passing through the origin.

In the more general case of a distribution in both activation entropy and enthalpy, i.e. a distribution in thermally activated free energy barriers, one needs to make an additional assumption regarding the relationship between the two distributions. One such assumption is that both ΔS and ΔH depend linearly on some other system variable p , that itself has a Gaussian distribution with mean p_m and width σ_p . This variable might, for example, be average intermolecular distance. If these relationships are expressed by

$$\Delta S = c + up \quad \Delta H = d + vp \quad (10)$$

then

$$\Delta S_m = c + up_m \quad \Delta H_m = d + vp_m \quad (11)$$

with c , d , u , and v constants. By using eqs 6, 8, 10, and 11, one obtains

$$\sigma_G = \frac{\sigma_H}{R} \left| \frac{1}{T} - \frac{u}{v} \right| = \left| \frac{\sigma_H}{RT} - \frac{\sigma_S}{R} \right| \quad (12)$$

where $\sigma_S = \sigma_H |u/v|$ is the width of the distribution of activation entropies. Note that in the special case where $c = d = 0$, the ratio u/v as obtained from $\Delta S_m / \Delta H_m$ must be equal to the value obtained from σ_S / σ_H . This can be an important test of the self-consistency of the analysis of the temperature dependence of relaxation times in terms of the Eyring model.

Another case to consider is the situation in which entropy and enthalpy are completely independent and their distributions are not related to each other via some other system variable. In this case, it can be shown that¹⁹

$$\sigma_G = [(\sigma_S/R)^2 + (\sigma_H/RT)^2]^{1/2} \quad (13)$$

Equation 13 cannot be used to fit the experimental data without the use of physically unrealistic imaginary values for σ_S/R . In all cases, the most probable relaxation time is given by

$$\ln(\tau_m) = \ln(2\pi h/kT) - \Delta S_m/R + \Delta H_m/RT \quad (14)$$

where m refers to the most probable value. In the case where no distribution is present in either ΔS or ΔH , as expected $\Delta S_m = \Delta S$ and $\Delta H_m = \Delta H$.

In real polymer systems the situation is complicated by slow changes in the specific volume,²³ the enthalpy,²⁴ or other system properties. These relaxation processes are referred to as structural relaxation, physical aging, stabilization, or annealing. The area has recently been reviewed by Hodge.²⁵ Several approaches have been used to take aging processes into account. The approach that we use here was proposed by Narayanaswamy.²⁶ In this approach, one treats the polymer relaxation at a temperature T , below the glass transition temperature, as if it consisted of two parts; a fraction x at equilibrium at temperature T and a fraction $(1 - x)$ at equilibrium at a fictive temperature T_f . In place of eq 6, one then writes the Eyring equation as

$$\ln \tau = \ln(2\pi h/kT) - \Delta S/R + x\Delta H/RT + (1 - x)\Delta H/RT_f(t_a) \quad (15)$$

where $T_f(t_a)$ is the fictive temperature which is a function of annealing time t_a . x is a partitioning parameter that divides ΔH into the two parts described above. As the annealing time increases $T_f(t_a) \rightarrow T$ and eq 15 \rightarrow eq 6. It is clear that whenever a distribution in ΔH is present and eq 15 describes the dependence of the decay time on annealing time, then the distribution parameter σ_G will also be dependent on annealing time. We can consider the same cases as before:

for a distribution in ΔH alone

$$\sigma_G = \sigma_H [x/RT + (1 - x)/RT_f(t_a)] \quad (16)$$

for a distribution in both entropy and enthalpy, where both quantities are dependent on a third material parameter

$$\sigma_G = \frac{\sigma_H}{R} [x/T + (1 - x)/T_f(t_a) - u/v] \quad (17)$$

and if enthalpy and entropy are completely independent

$$\sigma_G = \{(\sigma_S/R)^2 + [\sigma_H(x/RT + (1 - x)/RT_f(t_a))]^2\}^{1/2} \quad (18)$$

In all cases, the most probable relaxation time is

$$\ln(\tau_m) = \ln(2\pi h/kT) - \Delta S_m/R + \Delta H_m [x/RT + (1 - x)/RT_f(t_a)] \quad (19)$$

Note that in the first two cases, σ_G and $\ln(\tau_m)$ depend in exactly the same way on aging time t_a . This relationship will be shown to occur for the experimental data presented below.

III. Experimental Section

The guest–host polymer system used in this study consists of the optically nonlinear chromophore lophine-1 dissolved in the commercially available soluble poly(ether imide) Ultem. This system has been used and described in several previous poled-order relaxation studies.^{6,27} Chromophore and undoped polymer were dissolved together in anisole, and the solution was filtered and spin-coated onto indium tin oxide (ITO) coated quartz substrates, yielding good optical quality films (2–4 μm thick). The polymer-coated substrates were placed in an oven at about 170 °C for 2 h to remove residual solvent. The concentration of chromophore in the polymer host was 20 wt %, and the glass transition temperature as measured by differential scanning calorimetry (DSC) was 174 °C. No indication of phase separation in the polymer samples was observed.

The side-chain polymer was PMMA–DR1, frequently used as a model system to study polymer relaxations.⁴ Thin films of good optical quality were prepared by a procedure similar to the one described for the guest–host system. The chromophore concentration in this polymer was 25 wt % and the glass transition temperature as determined from DSC was 131 °C.

Two types of poling techniques, contact electrode and corona, were used for the guest–host system. The PMMA–DR1 samples were all corona poled. For the contact electrode poling experiments two polymer/ITO-coated quartz plates were fused together in a sandwich configuration by placing them together in an oven held at a temperature slightly above T_g . Electric fields obtained in these contact poling experiments were typically 50 V/ μm . For the corona poling experiments, a grid was used to control the positive surface potential of the sample. Fields of up to 200 V/ μm could be achieved in this way.

Before poling, the previous thermal history of the polymer film was erased by heating above the glass transition temperature for $1/2$ h. After poling, the sample was cooled quickly to the temperature where measurements were to be made and the electric field removed. In the corona poling experiments, the samples were poled a few degrees below T_g , until complete poling was achieved as determined by a leveling off in intensity of the poling-induced SHG (typically after about 20 min). The poling process was continuously monitored by recording the SHG signal from the samples. After removal of the positive surface charges by wiping the polymer surface with ethanol, the SHG decay was monitored for an appropriate length of time. In general, the same procedure was used with electrode poled samples. In this case, charges were removed, after poling and bringing the sample to the measurement temperature, by shorting the high-voltage electrodes.

Annealing experiments were performed on the guest–host system, using the electrode-poling technique. After poling slightly above T_g to avoid annealing effects during poling, the samples were cooled quickly to the temperature where the annealing and subsequent orientational decay was to be monitored. Annealing took place with the electric field on. In our experiments, the annealing temperature was 135 °C and annealing times ranged from 0 to 5 h.

The light source used in the SHG experiments was a CW diode pumped Q-switched Nd:YLF laser operating at a wavelength of 1047 nm (10 ns pulse width; 500 Hz repetition rate). After passing through a polarizer, the beam was focused onto

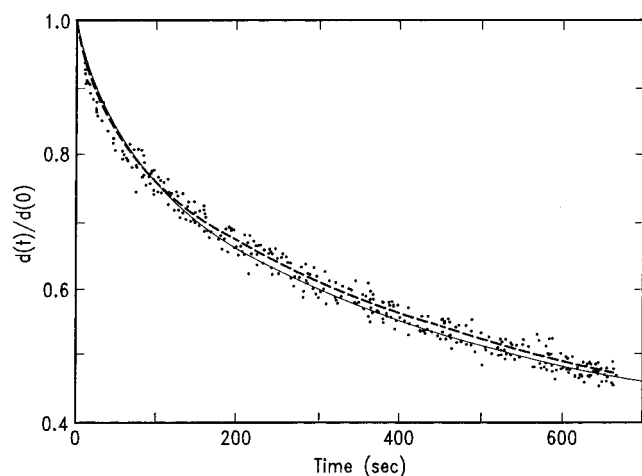


Figure 1. Decay of $d(t)/d(0) = [I(t)/I(0)]^{1/2}$ for 20 wt % lophine-1 in Ultem at 157 °C. The solid line is a fit of the data to the lognormal decay function eq 4, and the dashed line, a fit to the Kohlrausch-Williams-Watts function, eq 1.

the sample. The generated SHG signal was isolated by means of an IR filter and an interference filter and analyzed using a boxcar integrator. To improve the signal to noise ratio, the SHG from the polymer film was referenced to the signal from the quartz sample on a shot-by-shot basis.

The decay of the orientation was monitored at several temperatures for corona and contact poled samples. No dependence of the decay characteristics on the strength of the poling field was observed, and this agrees with the fact that very similar decay curves were observed for both poling techniques at a given temperature. For measurements near T_g , as much as 90% of the decay curve was followed; for the slowest relaxation decay processes (the lowest temperatures), as little as 5% of the decay was measured. All decays were measured within a time window short enough so that annealing effects could be ignored. Relaxation times determined from orientational decays for different samples of the same polymer at the same temperature were found to be reproducible to within about 20%. The reproducibility of the widths of the lognormal distribution was even better and found to vary by no more than 10%. The values of the width and relaxation time measured were not found to vary significantly when the same decay curve was fit over different time ranges.

IV. Discussion

A. Fitting of the Decay Curves. Figure 1 shows a typical decay of the square root of the normalized SHG signal ($\Phi(t)$ in eq 2). These data were fit using eq 4 derived from the lognormal model. Also shown is a fit to the stretched exponential or KWW function, eq 1. The figure indicates clearly the difficulty one has in distinguishing between these two functional forms from the experimental SHG decay data alone. As a matter of fact, we observed that all of the functional forms mentioned earlier^{4,6-10} can be used to fit the data. This is a well-known problem in the study of relaxation processes in amorphous systems. Unless one makes measurements over a very broad dynamic range in the decaying variable, one cannot distinguish among relaxation functions.¹¹ The lognormal functional form, eq 4, has been used in analyzing the data presented here for several reasons: (1) it is mathematically reasonably simple to work with and involves only two adjustable parameters, (2) the adjustable parameters can be related to physically meaningful thermodynamic quantities, (3) the temperature dependence of the adjustable parameters can be predicted, and (4) physical aging can easily be incorporated into the decay process.

Since the stretched exponential or KWW form, eq 1, is very widely used to describe relaxation processes in

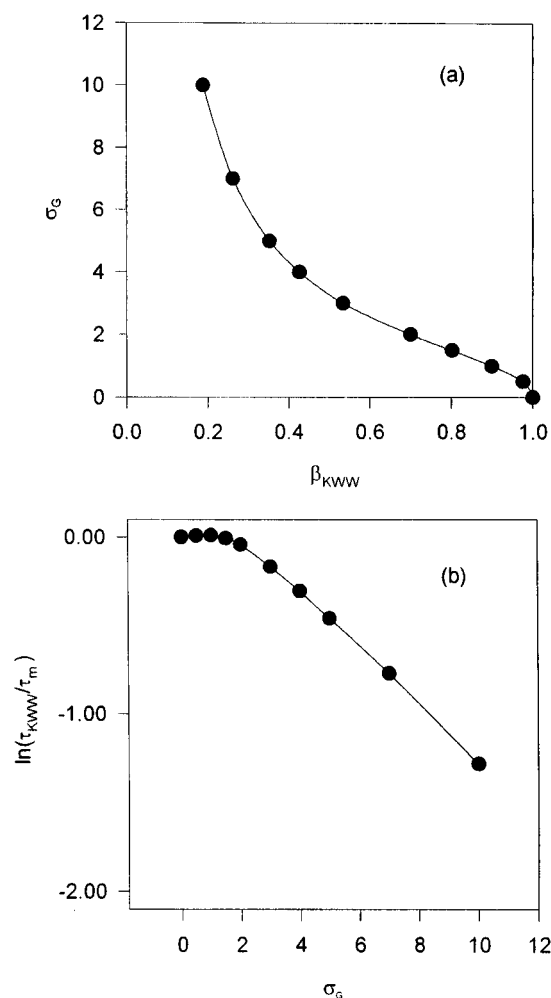


Figure 2. (a) Comparison of σ_G obtained using eq 4 and β_{KWW} obtained using eq 1 to fit the same hypothetical decay data. The hypothetical data were assumed to be an exact lognormal decay and the KWW function was used to fit these data for various values of σ_G (see text). (b) Values of $\ln(\tau_{KWW}/\tau_m)$ vs σ_G obtained from the fitting of the same data.

amorphous systems, it is useful to try to determine the relationship between the parameters found using that function with those obtained using the lognormal function. This will permit us to compare activation entropies and enthalpies obtained from the lognormal model with literature values obtained using the KWW function. Such a comparison is shown in Figure 2. In the figure, β_{KWW} and $\ln(\tau_{KWW}/\tau_m)$ are both correlated with σ_G . The data points were obtained by fixing τ_m at 1, varying σ_G , and fitting the resulting decay function for each σ_G value to the KWW function. It is important to point out that values obtained from these least squares fits depend on the time range over which the fitting procedure is carried out. This is of course due to the fact that we are comparing different mathematical functions. Here the fitting was carried out to $t = \tau_m$. From Figure 2a it is clear the β_{KWW} is inversely related to σ_G ; i.e. as β_{KWW} goes from 0 to 1 (pure exponential decay), σ_G goes from ∞ to 0. Figure 2b shows the logarithm of the ratio of τ_{KWW} to τ_m for different values of σ_G . For small values of σ_G ($\sigma_G \leq 2$; corresponding to $\beta_{KWW} \geq 0.6$), the relaxation times obtained are nearly equal, $\tau_m \approx \tau_{KWW}$. Even for larger values of σ_G , the τ 's do not vary significantly when compared to the several orders of magnitude variation in τ observed with temperature and to the experimental scatter in the τ values obtained for a given temperature. This means that

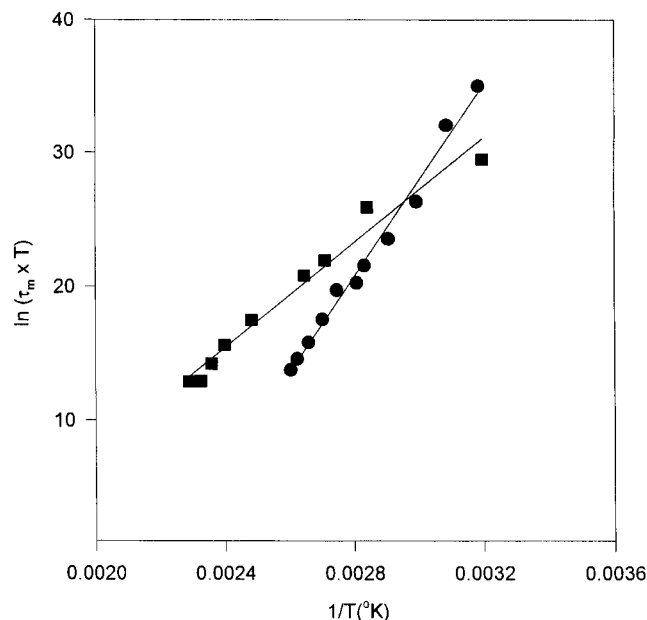


Figure 3. Plots of $\ln(\tau_m T)$ vs $1/T$ for PMMA-DR1 (●) and lophine-1 in Ultem (■). The solid line is a linear least squares fit through the data points.

activation energies obtained from measurements of τ (T), using either function to fit the experimental decay data, should be equal within experimental uncertainties and one can make meaningful comparison between experimental data analyzed using the KWW and log-normal decay functions.

B. Temperature Dependence of Relaxation Parameters. If orientational decay in NLO polymers can be described by a Gaussian distribution of free energy barriers, then, according to eq 14, a plot of $\ln(\tau_m T)$ vs $1/T$ should yield a straight line with slope related to the mean value of the enthalpy ΔH_m . From Figure 3, one sees that the decay data for both guest–host and side-chain polymers are consistent with the predicted temperature dependence. As a consequence, one can directly calculate mean activation entropies and enthalpies from the temperature dependences of the most probable relaxation time using eq 14. From the results reported in Figure 3, we obtain activation enthalpies of 39 ± 7 kcal/mol for the lophine-1–Ultem guest–host polymer and 71 ± 10 kcal/mol for the side-chain PMMA-DR1 polymer. These values are within the range of values found in other studies of orientational relaxations in NLO polymers.²⁸ These other studies used the KWW function and the Arrhenius equation (eq 5) to determine relaxation times and activation energies, but as we have pointed out, these values should be in reasonable agreement with activation enthalpies obtained using the lognormal decay function to describe the experimental data. Activation entropies were found to be 19 ± 6 and 115 ± 28 cal/(K·mol) for lophine-1–Ultem and PMMA-DR1, respectively. These large positive entropies (and enthalpies) are not unusual for polymer systems²¹ and are often associated with a relaxation mechanism involving complex cooperative interactions among polymer subunits.²² (The error margins quoted above are standard errors assuming that eq 14 correctly describes the data.)

The temperature dependence of σ_G is shown in Figure 4. σ_G varies significantly with temperature for both polymer systems, indicating, in the model used here, a broadening of the distribution of relaxation times with decreasing temperatures. Recall that this broadening

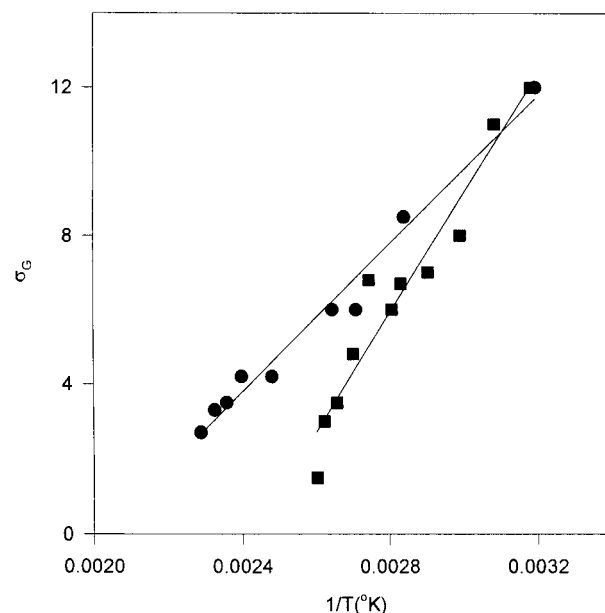


Figure 4. Plots of σ_G vs $1/T$ for PMMA-DR1 (■) and lophine-1 in Ultem (●). The solid line is a linear least squares fit through the data points.

Table 1. Relationship among Experimentally Determined Thermodynamic Quantities (All Values in Units of K^{-1})

	$\Delta S_m/\Delta H_m$ ($\times 10^{-3}$)	$\beta S/\beta H$ ($\times 10^{-3}$)	α ($\times 10^{-4}$)	$\Delta S_m/4\Delta H_m$ ($\times 10^{-4}$)
PMMA-DR1	1.6 ± 0.4	2.4 ± 1.5	2.6^a	4.0 ± 1.6
lophine-1–Ultem	0.5 ± 0.2	2.0 ± 1.1	1.1^b	1.2 ± 0.5

^a Wunderlich, W. In *Polymer Handbook*; Brandrup, J., Immergut, E. H., Eds.; John Wiley and Sons: New York, 1989; p V/77.

^b Pecht, M.; Wu, X. *IEEE Trans. Compon. Packag. Manuf. Technol. B* **1994**, 17, 632. Average of in-plane and out-of-plane coefficients.

is due to the presence of underlying distributions of activation enthalpies and entropies which are themselves temperature independent. Both guest–host and side-chain data are satisfactorily described by eq 12, indicating the presence of a nearly Gaussian distribution in both activation entropy and enthalpy. Equation 12 also implies that ΔS and ΔH are linearly related to a common system variable that itself has a Gaussian distribution. In addition we noticed in Table 1 that the ratio $\Delta S_m/\Delta H_m$ is of the same order of magnitude as σ/σ_H , indicating that enthalpy and entropy are, at least approximately, directly proportional to a single variable p (i.e. c and d in eq 10 are approximately zero).

Another way of evaluating the internal consistency of the activation entropies and enthalpies found from using the temperature dependence of the orientational relaxation parameters is to use empirical relationships that relate activated volumes to thermodynamic quantities. Eby²⁹ has suggested using the following two relationships^{30,31}

$$\Delta V = \beta/\alpha\Delta S \quad (20)$$

and

$$\Delta V = 4\beta\Delta H \quad (21)$$

to obtain a third relationship that does not contain the activated volume ΔV :

$$\Delta S/\Delta H = 4\alpha \quad (22)$$

In these equations, β is the isothermal compressibility

(not to be confused with the subscripted β_{KWW} used earlier as a parameter in the stretched exponential decay function eq 1) and α is the isobaric coefficient of thermal volume expansion. If eq 22 is valid for the NLO polymers considered here, then the chromophore relaxation process can be related to a distribution in activation volume. Table 1 shows a comparison between measured values of α for pure PMMA and Ultem and values obtained from the chromophore relaxation data using eq 22. The agreement is really quite good, particularly when one notes that the thermal expansion coefficient is measured in pure polymers and the relaxation data are measured in polymers heavily doped with chromophore molecules. Another point of comparison is to use eq 21 along with a knowledge of the isothermal compressibility α to calculate the activated volume ΔV . Using the value of β for PMMA from ref 29 for PMMA-DR1, one obtains a value of 705 cm³/mol for ΔV in rough agreement with a value of 1427 cm³/mol obtained using eqs 20 and 21 and activated energies and enthalpies from dynamic mechanical analysis.²⁹ The value is not in such good agreement with the one obtained by Brower and Hayden³² from measurements of the pressure dependence of the chromophore orientational relaxation time for the guest-host system DR1 in PMMA. These authors obtained a value of 86 cm³/mol for ΔV .

Several authors have successfully fit temperature dependences of average relaxation time obtained using eq 1 to non-Arrhenius functional forms.^{6,33} Using eq 4 to fit the data, we have found no substantial deviations from Arrhenius behavior for the limited number of samples examined.

The effects of physical aging in the guest-host polymer lophine-1-Ultem on the relaxation parameters τ_m and σ_G are shown in Figure 5 for aging and relaxation at 135 °C. After an initial period of several minutes within which neither parameter changes significantly, both quantities increase with increasing aging time t_a . It is also clear that both τ_m and σ_G show a similar functional dependence on aging time, as predicted by the simple aging model described by eqs 16, 17, and 19. This is shown more clearly in Figure 6 where the straight line in a plot of $\ln \tau_m$ vs σ_G indicates the similarity in the functional dependence of these two quantities on aging time.

V. Conclusion

The results presented in this paper indicate that poled-order relaxation in NLO polymers can be adequately described by a model based on a Gaussian distribution in the logarithm of the relaxation times. This functional form allows one to obtain physically meaningful thermodynamic quantities from the experimental data. Activation enthalpies, entropies, and volumes along with the widths of the Gaussian distributions in these quantities can be obtained from the SHG decay data, and these quantities can be compared among themselves for internal consistency and can be related to independently measured values for other quantities, such as thermal expansion coefficients. Physical aging can also be described within this model. Data for guest-host and side-chain polymer systems are analyzed in this way and the lognormal distribution has been found to describe the results adequately. The agreement we observe between the predictions of the model based on a Gaussian distribution of activation energies and enthalpies should not be interpreted as

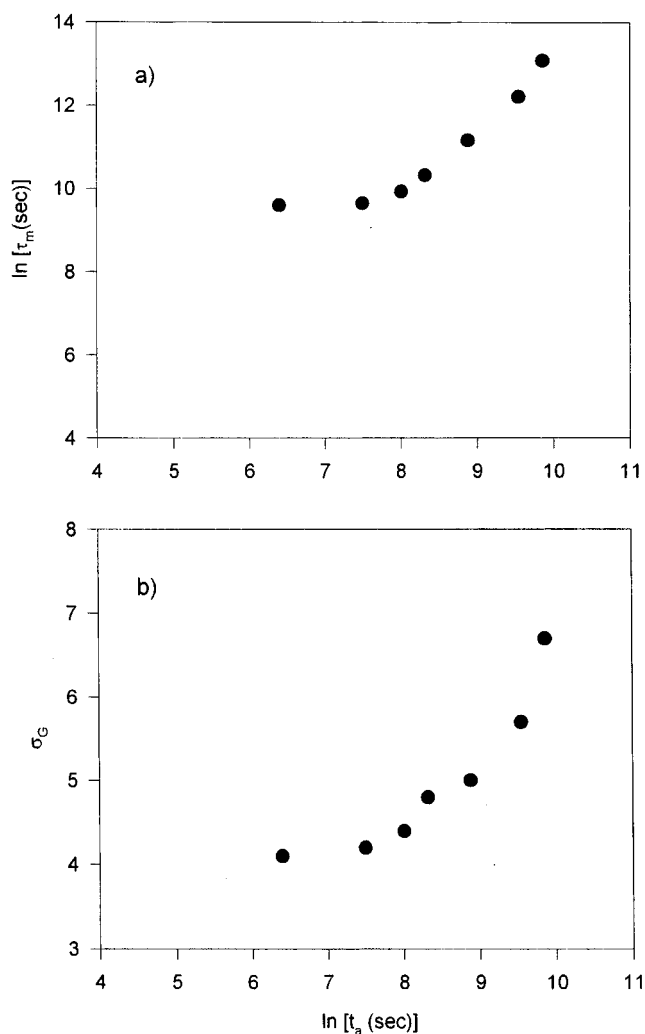


Figure 5. Plots of $\ln \tau_m$ (a) and σ_G (b) vs $\ln t_a$ for lophine-1 in Ultem. The annealing temperature was 135 °C. The orientational relaxation was also measured at 135 °C.

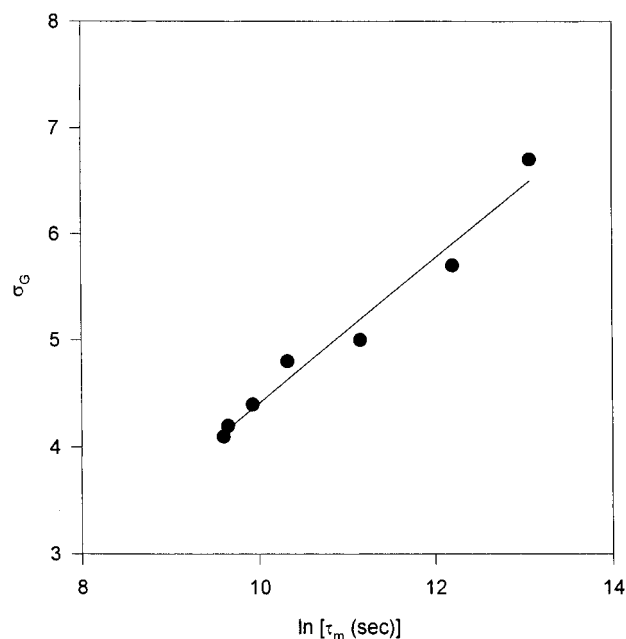


Figure 6. Each of the data points represents a measured σ_G and $\ln \tau_m$ for the same aging time t_a for lophine-1 in Ultem, meaning that the distributions are precisely Gaussian and symmetric. Other functional forms for these distributions could perhaps also be used to describe the

relaxation process. Nor should values of τ_m greater than 3000 s be taken to indicate precise values for the characteristic relaxation time. There are two reasons for this. First, the decay measurements are made over a time that is only a small fraction of τ_m and the error margins in the determination of τ_m become larger for longer decay times. Second, as Figure 5 shows, annealing effects begin to affect the measured values at longer times. Nevertheless, the thermodynamic quantities determined from plots such as those in Figures 4 and 5 are not significantly different when only data for decay times less than 3000 s are used.

Bendler and Shlesinger¹⁴ have shown that the stretched exponential function, eq 1, can be obtained from an asymmetric exponential distribution in activation enthalpies and entropies. They assume a linear relationship between these two quantities, equivalent to our assumption that $c \approx d \approx 0$. They then obtain the following relationship for the temperature dependence of the stretched exponential β_{KWW} :

$$\beta_{KWW} = akT/(1 - bT) \quad (23)$$

where a and b are constants. This expression, which goes to zero as T approaches zero, does not fit experimentally measured values of β_{KWW} as a function of temperature, even though the stretched exponential function itself does fit the decay data. This would seem to imply either that the actual distribution of activation enthalpies and entropies is closer to the symmetric Gaussian than the asymmetric exponential functional form or that the approximation that $c \approx d \approx 0$ is not valid. The data presented here cannot distinguish these two possibilities.

Determination of the exact functional relationship for the decay of electric field induced polar order in polymers awaits experimental measurements over a much greater fraction of the decay process than has previously been done. Such measurements may be complicated by structural relaxations, i.e. aging processes, that are simultaneously occurring and that will influence the observed relaxation process.

Acknowledgment. This work has benefited greatly from discussions and collaborations with G. Bjorklund, C. Moylan, R. Miller, R. Twieg, and W. Volksen. T.V. was a postdoctoral researcher of the Belgian National Fund for Scientific Research (NFWO). We would like to acknowledge support from the Commission for Educational Exchange between the U.S.A., Belgium, and Luxembourg and from IBM Belgium. This work has been supported in part by the Advanced Research Projects Agency (Grant No. MDA972-93-1-0007) and by the National Institute of Standards/Advanced Technology Program (Cooperative Agreement No. 70NANB2-H1246).

References and Notes

- (1) Burland, D. M.; Miller, R. D.; Walsh, C. A. *Chem. Rev.* **1994**, *94*, 31.
- (2) Hampsch, H. L.; Yang, J.; Wong, G. K.; Torkelson, J. M. *Macromolecules* **1990**, *23*, 3640, 3648.
- (3) Köhler, W.; Robello, D. R.; Dao, P. T.; Willand, C. S.; Williams, D. J. *J. Chem. Phys.* **1990**, *93*, 9157.
- (4) Singer, K. D.; King, L. A. *J. Appl. Phys.* **1991**, *70*, 3251.
- (5) Chung, S. H.; Steven, J. R. *Am. J. Phys.* **1991**, *59*, 1024.
- (6) Stäbelin, M.; Walsh, C. A.; Burland, D. M.; Miller, R. D.; Twieg, R. J.; Volksen, W. *J. Appl. Phys.* **1993**, *73*, 8471.
- (7) Lindsay, G. A.; Henry, R. A.; Hoover, J. M.; Knoesen, A.; Mortazavi, M. A. *Macromolecules* **1992**, *25*, 4888. Suzuki, A.; Matsuoka, Y. *J. Appl. Phys.* **1995**, *77*, 965.
- (8) Goodson, T., III; Wang, C. H. *Macromolecules* **1993**, *26*, 1837.
- (9) Wang, L.; Zhang, Y.; Yamakado, M.; Wada, T.; Sasabe, H. *Mol. Cryst. Liq. Cryst.* **1994**, *255*, 131.
- (10) Wang, H.; Jarnagin, R. C.; Samulski, E. T. *Macromolecules* **1994**, *27*, 4705.
- (11) Beckmann, P. A. *Phys. Rep.* **1988**, *171*, 85. Böttcher, C. J. F.; Bordewijk, P. *Theory of Electric Polarization*; Elsevier Science Publishers: Amsterdam, 1978; Vol. II, pp 45–92.
- (12) Dhinojwala, A.; Wong, G. K.; Torkelson, J. M. *Macromolecules* **1993**, *26*, 5943. Dhinojwala, A.; Hooker, J. C.; Torkelson, J. M. *J. Non-Cryst. Solids* **1994**, *172–174*, 286.
- (13) Kaminow, I. *An Introduction to Electrooptic Devices*; Academic Press: New York, 1974; p 56.
- (14) Schlesinger, M. F.; Montroll, E. W. *Proc. Natl. Acad. Sci. U.S.A.* **1984**, *81*, 1280. Motroll, E. W.; Bendler, J. T. *J. Stat. Phys.* **1984**, *34*, 129. Bendler, J. T.; Shlesinger, M. F. *Macromolecules* **1985**, *18*, 591.
- (15) Shore, J. E.; Zwanzig, R. *J. Chem. Phys.* **1975**, *63*, 5445. Skinner, J. L. *J. Chem. Phys.* **1983**, *79*, 1955.
- (16) Richert, R. *Macromolecules* **1988**, *21*, 923; *Chem. Phys.* **1988**, *122*, 455. Schüssler, S.; Richert, R.; Bässler, H. *Macromolecules* **1994**, *27*, 4318; **1995**, *28*, 2429.
- (17) Verbiest, T.; Burland, D. M. *Chem. Phys. L.*, in press.
- (18) Wiechert, E. *Ann. Phys.* **1993**, *50*, 335, 546. Wagner, K. W. *Ann. Phys.* **1913**, *40*, 817.
- (19) Nowick, A. S.; Berry, B. S. *IBM J.* **1961**, October, 297.
- (20) Jahnke, E.; Emde, F. *Table of Higher Functions*, 4th ed.; Dover: New York, 1948; pp 38–39.
- (21) Kauzmann, W. *Rev. Mod. Phys.* **1942**, *14*, 12.
- (22) Starkweather, H. W., Jr. *Macromolecules* **1981**, *14*, 1277.
- (23) Matsuoka, S.; Williams, G.; Johnson, G. E.; Anderson, E. W.; Furukawa, T. *Macromolecules* **1985**, *18*, 2652. Rendell, R. W.; Ngai, K. L.; Fong, G. R.; Aklonis, J. J. *Macromolecules* **1987**, *20*, 1070.
- (24) Hodge, I. M. *Macromolecules* **1987**, *20*, 2897. Cowie, J. M. G.; Ferguson, R. *Macromolecules* **1989**, *22*, 2307, 2312.
- (25) Hodge, I. M. *J. Non-cryst. Solids* **1994**, *169*, 211; *Science* **1995**, *267*, 1945.
- (26) Narayanaswamy, O. S. *J. Am. Ceram. Soc.* **1971**, *54*, 491.
- (27) Stäbelin, M.; Burland, D. M.; Ebert, M.; Miller, R. D.; Smith, B. A.; Twieg, R. J.; Volksen, W.; Walsh, C. A. *Appl. Phys. Lett.* **1992**, *61*, 1626. Walsh, C. A.; Burland, D. M.; Lee, V. Y.; Miller, R. D.; Smith, B. A.; Twieg, R. J.; Volksen, W. *Macromolecules* **1993**, *26*, 3720.
- (28) van der Vorst, C. P. J. M.; van Rheede, M.; van Weerdenburg, C. J. M. *Int. J. Polym. Mater.* **1993**, *23*, 113. Zysset, B.; Ahlheim, M.; Stäbelin, M.; Lehr, F.; Prêtre, P.; Kaatz, P.; Günter, P. *Proc. SPIE* **1993**, *70*, 2025. Chen, J. I.; Marturunkakul, S.; Li, L.; Jeng, R. J.; Kumar, J.; Tripathy, S. K. *Macromolecules* **1993**, *26*, 7379.
- (29) Eby, R. K. *J. Chem. Phys.* **1962**, *37*, 2785.
- (30) Keyes, R. W. *J. Chem. Phys.* **1958**, *29*, 467.
- (31) Lawson, A. W. *J. Phys. Chem. Solids* **1957**, *3*, 250.
- (32) Brower, S. C.; Hayden, L. M. *Appl. Phys. Lett.* **1993**, *63*, 2059.
- (33) Man, H. T.; Yoon, H. N. *Adv. Mater.* **1992**, *4*, 159. Prêtre, P.; Kaatz, P.; Bohren, A.; Günter, P.; Zysset, B.; Ahlheim, M.; Stäbelin, M.; Lehr, F. *Macromolecules* **1994**, *27*, 5476.

MA960179R